

A PRACTICAL MICROWAVE TRAVELLING-WAVE MESFET
GATE MIXER

O.S.A. Tang and C.S. Aitchison*,

Department of Electronics, Chelsea College, London University
Pulton Place, London SW6 5PR, U.K.
*now with ERA Technology Ltd, Leatherhead, Surrey, U.K.

Abstract

The theoretical analysis of Travelling-Wave (Distributed) Mixing is briefly described. Experimental verification on a 2-section design, comparing theoretical and measured results is presented for the first time. The tradeoffs between circuit variables are briefly explained. It exhibits around 4dB of conversion loss over the signal frequency band from below 2GHz to 10GHz for an I.F. of 1.5GHz.

Introduction

Microwave MESFET mixers (2),(3) are useful alternatives to conventional diode mixers because they offer conversion gain instead of conversion loss. However, until now, only narrow band MESFET resonant mixers have been reported. In an attempt to make a truly wide-band MESFET mixer, the concept of Travelling Wave or Distributed Mixing was proposed by the authors(1) in 1984. The main objectives of this paper are to demonstrate the principle practically and to describe briefly a more generalized theory for hybrid design than that given in (1).

Theory

Essentially, the concept of distributed mixing is based on the principle of distributed amplification (4). The unilateral simplified model of a Travelling Wave mixer realised in discrete hybrid form using single gate MESFETs and consisting of 50ohms input and output lines is illustrated schematically in Fig. 1. R_{ds1} , C_{gs} and g_{mi} are assumed to be the dominant non-linearities (2) that yield mixing under the modulation effect of the large signal local oscillator (L.O.) and especially g_{mi} in the case of a single gate mixer configuration considered here. The external wideband directional coupler can be dispensed with if dual gate MESFETs are used instead, and in which case two separate gate lines will be required. It is assumed that resistive losses in the source grounding path are absorbed into R_{gs1} and R_{md1} in Fig. 1, while associated parasitic inductances are absor-

ed into L_{mg} and L_{md} , which represent the effective bond wire inductances in the gate and drain respectively.

A simplified non-linear model of the NEC NE 71000 GaAs MESFET chip under large L.O. signal has been developed. It is based on D.C. and low frequency (2MHz) characterization, as well as small signal 2 to 18GHz S-parameters measurements at two different bias points (0.3 I_{DSS} and 0.8 I_{DSS}). The small signal bilateral equivalent circuit at 0.3 I_{DSS} and 0.8 I_{DSS} is depicted in Fig. 2. The bias dependence of g_m , C_{gs} and R_{ds} is measured by D.C. I-V characteristics and low frequency characterization. Cubic Spline curve fitting and Fast Fourier Transform are applied to evaluate their frequency spectrum components. The variation of the 1st harmonic of $g_m(t)$ and the D.C. component of $R_{ds}(t)$ with local oscillator amplitude under different gate bias conditions inside the current saturation region is illustrated in Fig. 3 and Fig. 4 respectively.

The analysis presented in (1) did not take into account the presence of L_{mg} , L_{md} , lossy grounding path or non-ideal coaxial to microstrip launcher. Moreover, R_{ds} is assumed to be linearly dependent on gate bias. The analytical model has now been improved to remove these approximations.

The complete theoretical analysis will be given in a future paper and so only the salient parts of the Conversion Gain formula are given here. The conversion gain, G , of an n -section Travelling Wave mixer is approximately given by

$$\frac{1}{4} \left| \Delta^*(f_{RF}) \right|^2 \left| \zeta(f_{RF}, f_{LO}, f_{IF}) \right|^2 \psi(f_{RF}, f_{LO}, f_{IF}) \cdot \frac{\text{Re}(Z_{DT}(f_{IF})) \left| Z_{in}^*(f_{RF}) \right|^2}{\text{Re}(Z_{in}^*(f_{RF}))}$$

and where $*$ represents the complex conjugate of a complex number, and $\Delta(f_{RF})$ concerns with the share of the total voltage across the gate that appears across C_{gs} . $\zeta(f_{RF}, f_{LO}, f_{IF})$ represents the effective I.F. current contributions from each of the current generator of the FET, while $Z_{DT}(f_{IF})$ and $Z_{in}(f_{RF})$ are input impedances illustrated in Fig.1. Finally, $\psi(f_{RF}, f_{LO}, f_{IF})$ deals with the effects of reflections in the two artificial transmission lines.

We have explored in (1) that the main dis-

advantages of MESFET's gate resistive loading are the drop in characteristic impedance as well as higher section attenuation near cutoff frequency as the number of sections is increased. It transpires that by increasing the gate line characteristic impedance, the ill-effects of resistive gate loading can be minimized within the passband of the gate line. However, for a given value of \bar{C}_{gs} of a chosen MESFET, increasing the d.c. characteristic impedance R_o will incur significant penalties such as reducing the final bandwidth f_{CG} of the line. For example, the relationship in an ideal lossless line is

$$f_{CG} = \frac{1}{\pi R_o \bar{C}_{gs}}$$

So in cases where MESFETs with relatively large \bar{C}_{gs} are employed and the required operating band extends to relatively high frequency, resort must be made to reducing R_o , in the interests of extending the final cutoff frequency of the line and reducing the resistive loading at the high frequency end of the required operating band. The degradation of Conversion Gain can be compensated by employing more sections in the design.

Experimental Verification

To demonstrate the concept and theory proposed a simple 2-section design has been realized in hybrid form, employing two NEC NE71000 GaAs MESFET chips. As a first attempt, our primary goal is not to design one with the maximum performance in mind, but to be able to easily verify the theory developed. Hence, the design comprises nominally 50ohm gate and drain lines together with an external directional coupler, and was fabricated on Alumina substrate. 25 μ m Gold bond wires were employed to simulate wideband lumped inductors while lumped capacitors to ground were realized using low impedance microstrip lines. Source grounding was provided by two ultrasonically drilled via-holes filled with silver loaded paint.

The variation of conversion loss with signal frequency for a constant I.F. of 1.5GHz is shown in Fig. 5. A conversion loss of 4(+1,-0.5) dB was demonstrated from 2 to 10GHz of R.F. (or 3.5 to 11.5GHz of L.O.), under -0.5V gate bias and 6dBm L.O. drive level. This is believed to be the lowest figure reported for wideband mixers covering such a signal bandwidth in this frequency range. Good agreement with predicted results is observed. The slight discrepancies beyond 10GHz were attributed mainly to internal feedback effects inside the MESFET, as well as parasitic feedback due to unsatisfactory Source grounding, which are not accounted for in the theory. If we are to attach greater importance to maximum achievable gain than flatness of characteristic, then the loss reduces further to 3(+1.5, -0.5)dB over the same frequency band under optimum gate bias and L.O. drive level at each signal frequency. Preliminary results show that the conversion gain will become positive if the I.F. is reduced below certain frequency value. For example, a measured conversion gain of +0.5dB (+0.5dB) was demonstrated from 2 to 10GHz of R.F. for an I.F. of 10MHz, as depicted in Fig. 5. The cause of this phenomenon is

still under investigation.

The effects of various circuit parasitics are also independently identified and investigated. In particular, internal FET gate losses, external gate bond wire inductance and losses in the Source grounding path are the dominant sources of gain reduction especially towards the high frequency end of the operating band.

A typical variation of calculated and measured Conversion Gain with L.O. power is shown in Fig. 6. Good agreement is observed up to 11dBm of L.O. power. The theory fails to predict the fall in Conversion Gain above 11dBm because two phenomena have been neglected in the theory. Firstly, an abrupt drop in R_{ds} will result if the drain L.O. voltage swings beyond the current saturation region. Secondly, with even higher L.O. power, the gate line turns from an LCR line to an LR line because of the shunting effect of forward biased leakage resistance across C_{gs} 's.

The 1dB compression point of this design occurs typically at around +5dBm with 11dBm of L.O. drive level. The I.F. output port exhibits a return loss of greater than 23dB while S11 of the input port, at the L.O. frequency with the directional coupler removed and with 6dBm of input power applied is displayed in Fig. 7.

In the light of the experience gained in this practical exercise, the design of a 4-section mixer employing 4 MESFETs as well as the investigation of the noise characteristics are currently in progress. Superior performance is anticipated.

Conclusion

A general theory of Travelling Wave Mixing adopted for discrete hybrid design has been developed. Performance data of a practical 2-section design are given and agree well with theoretical predictions.

Acknowledgements

Acknowledgement is made to Marconi Defence Systems Ltd., U.K. for their support of this work. The authors would also like to thank A.E. Ward of Marconi and Carlos Camacho-Penalosa of the Universidad Politecnica de Madrid (Spain) for helpful discussions.

References

- (1) O.S.A. Tang and C.S. Aitchison, "A Microwave Distributed MESFET Mixer" Conference Proceedings of the 14th European Microwave Conference, Belgium, Sept. 1984.
- (2) R.A. Pucel, D. Masse and R. Bera, "Performance of GaAs MESFET Mixers at X-Band" IEEE Trans. MTT-24, No.6, June 1976.
- (3) G.K. Tie and C.S. Aitchison, "Noise Figure and associated Conversion Gain of a Microwave MESFET Gate Mixer" Conference Proceedings of the 13th European Microwave Conference, West Germany, Sept. 1983.
- (4) W.S. Percival, "Thermionic Valve Circuits", British Patent 460562, 1937.

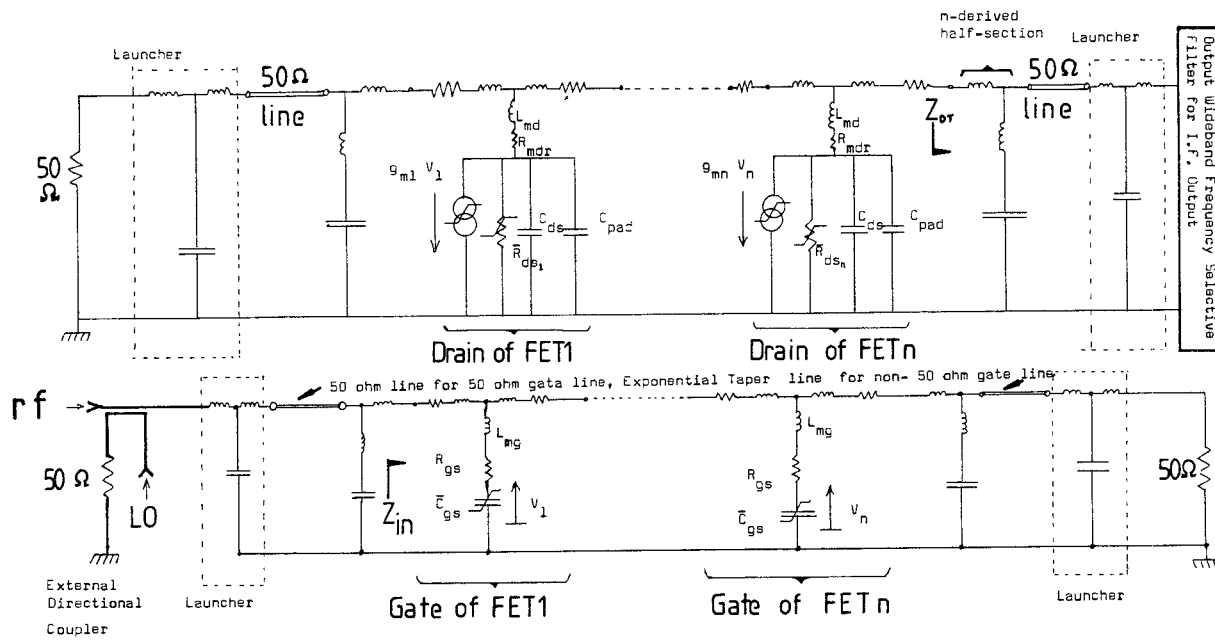


FIG 1 Equivalent Circuit of a Travelling Wave Mixer realized in discrete hybrid form and comprises of 50 ohm input Gate Line and 50 ohm output Drain Line (DC circuits not shown)

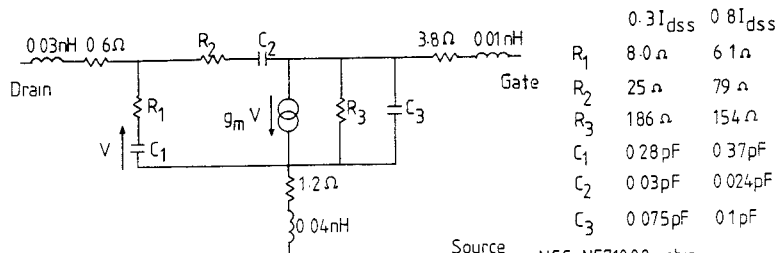


FIG 2 (2 to 18 GHz) small signal computer optimized equivalent circuit

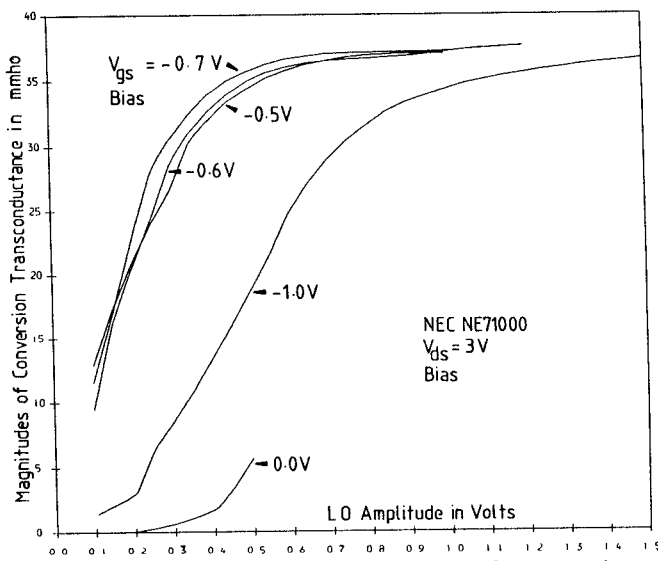


FIG 3 Variation of the magnitudes of Conversion Transconductance with LO Amplitude

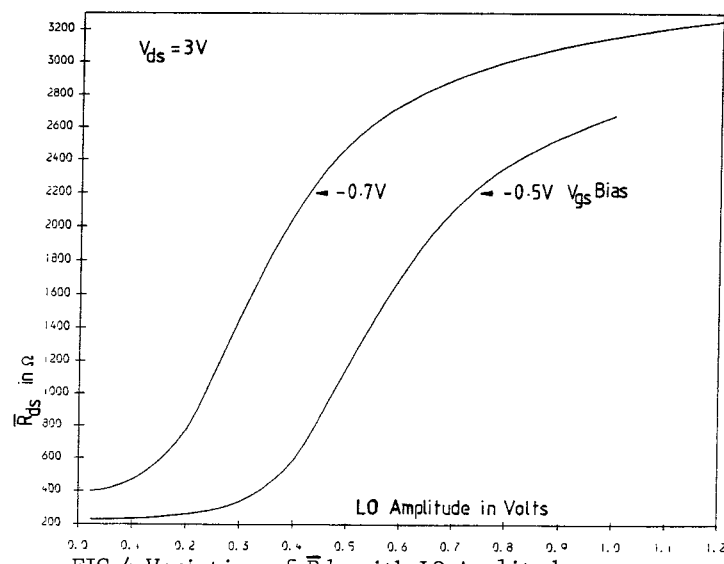


FIG 4 Variation of \bar{R}_{ds} with LO Amplitude

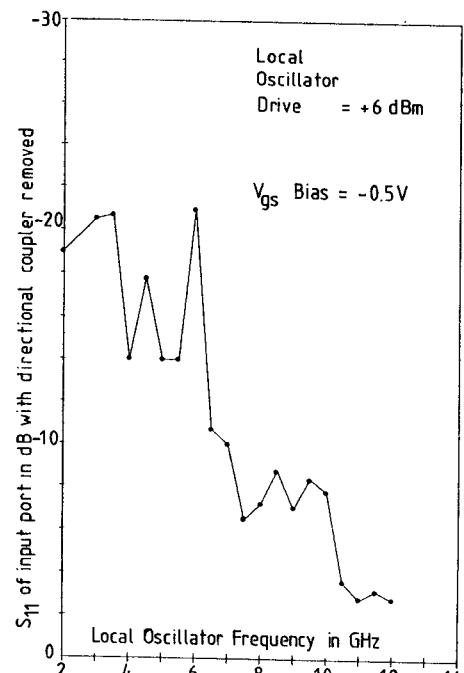


FIG 7 Variation of input port S11 with LO Frequency

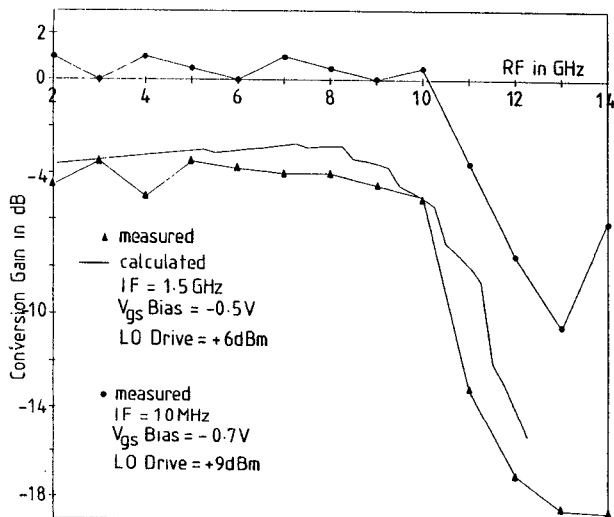


FIG 5 Variation of Conversion Gain with signal RF

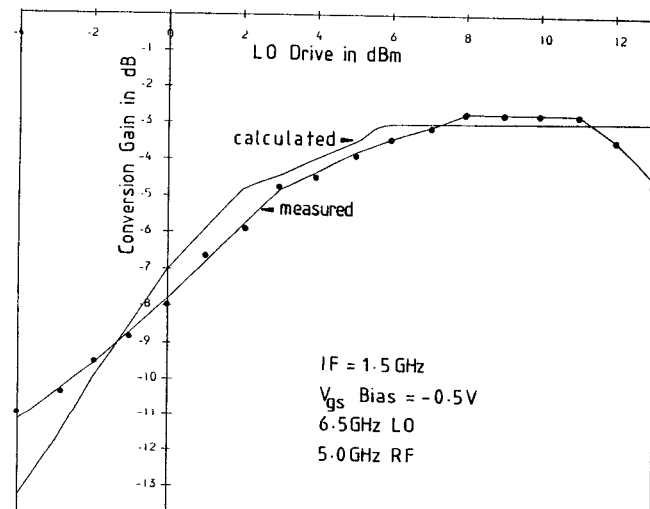


FIG 6 Variation of Conversion Gain with LO Drive Level